

# CHARACTERIZING THE NONLINEAR BEHAVIOR OF FLAKEBOARDS<sup>1</sup>

*Theodore L. Laufenberg*

Research General Engineer  
USDA Forest Service, Forest Products Laboratory, Madison, WI 53705

(Received 2 February 1982)

## ABSTRACT

To predict accurately the failure load of a layered flakeboard in bending, the stress-strain relations appropriate for each layer must be known. This paper describes the application of a method for characterizing the nonlinear behavior of a flakeboard material subjected to axial stresses. The model permits prediction of the stress-strain curve to the ultimate stress and ultimate strain points for the material regardless of fiber alignment or board density. Comparisons are made between traditional failure criteria, experimental results, and the model predictions.

*Keywords:* Flakeboards, failure in bending, model predictions, stress-strain relations.

Higher percentages of the structural sheathing market will be turning during the 1980s to the class of products known as flakeboards (Dickerhoof and McKeever 1980; Neill 1980). To be successful in the marketplace, these panels will need to be cost-competitive with veneered panels and have equal performance capabilities. With increased market competition between reconstituted panel products in the years ahead, the end-product properties and the available raw material will need to be matched closely. To optimize production processes, manufacturers of flakeboards will require a consistent method of predicting their materials' engineering properties.

Many researchers have presented techniques for predicting the strength or stiffness of flake and particle materials. Geimer's work (1980) is thorough in the use of empirical regressions to provide predictions of uniform-density-flakeboard properties as functions of density, alignment, species, and flake type. A finite-element model for prediction of the elastic constants of flakeboards was used by Hunt and Suddarth (1974) with encouraging results, but no attempt was made to predict the strength properties. Numerous other works, such as those of Brumbaugh (1960), Keylwerth (1958), Post (1961), and Simpson (1977), have had goals of providing reliable strength or stiffness relationships for use by the flakeboard industry.

In all of the research work done to date, no attempt has been made to quantify the stress-strain response to failure of flakeboards. The published MOE predictions certainly identify the linear elastic response of this material, but flakeboard is not elastic to failure (Fig. 1). Furthermore, to predict accurately the failure load of a layered flakeboard in bending, the stress-strain relationships must be known for each layer.

This paper describes a modeling technique, and its application, that allows prediction of the stress-strain behavior to failure of a flakeboard, of any density

---

<sup>1</sup> This article was written and prepared by a U.S. Government employee on official time and is therefore in the public domain.

or flake alignment, made with one flake type and subjected to axial loading. Regression equations for MOE and MOR formulated by Geimer (1980) are used in conjunction with the Ramberg-Osgood equation (1943) to generate the flakeboard response to failure. The commonly used linear elastic maximum strain failure criteria are compared with the Ramberg-Osgood characterization of maximum strain developed. Each of these methods of failure prediction is compared to experimentally determined failure strain data.

#### EXPERIMENTAL

All of the experimental data, the MOE, and the ultimate strength regressions used in this paper were generated by Geimer's (1980) research testing and evaluations.

Douglas-fir flakes were used to construct flakeboards at four target density levels (30, 40, 50, 60 lb/ft<sup>3</sup>) and four target fiber alignment values (0, 40, 60, 80%). The percentage of fiber alignment, AL, is defined as

$$AL = \frac{45^\circ - \theta}{45^\circ} \quad (1)$$

and

$$\theta = \frac{\sum_{f=1}^{f=m} \theta_f}{m}$$

in which  $\theta$  = average fiber angle from board-forming direction (degrees)

$\theta_f$  = individual fiber angle from board-forming direction (degrees)

$m$  = number of individual fiber angles measured

The flakes were disk-cut, 0.020 inch thick by 3 inches long, dried to 10% MC, and sprayed with 5% phenolic resin and 1% wax. All mats were pressed between cold platens to final density and subsequently heated so that the core temperature reached 235 F within 11 min. These procedures were used to achieve uniform-density material throughout the thickness of the boards, thus alleviating any need to address the effects of their density profiles upon mechanical properties.

Use of the sonic velocity measurement was investigated by Geimer as a means of determining the relative amount of flake alignment. This relationship was proposed:

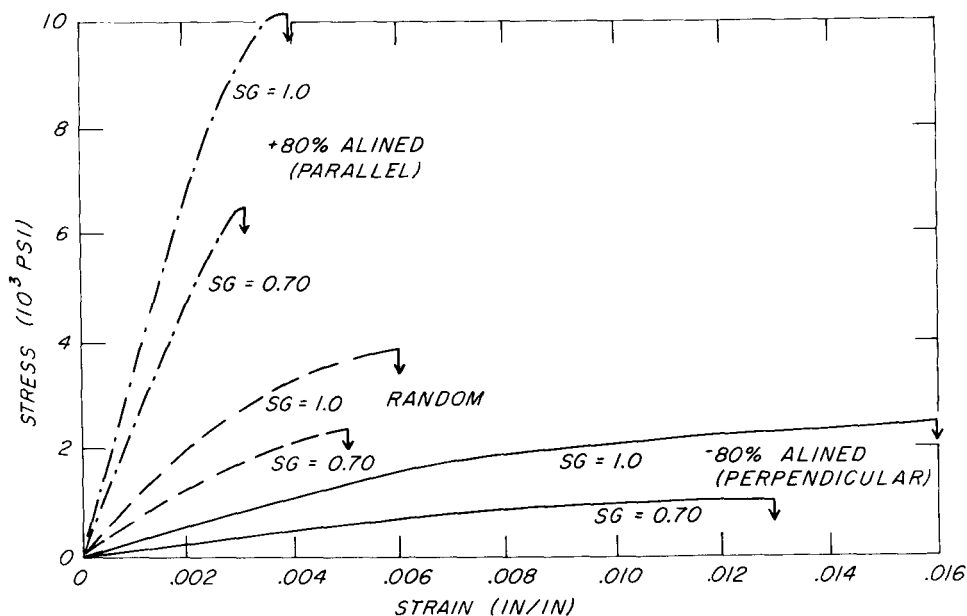
$$AL = A + B \ln(\text{SVR}) \quad (2)$$

in which AL = percentage of fiber alignment, as defined previously

A, B = constants in the regression equation

SVR = the ratio of the sonic velocity measurements in the board-forming direction, and the direction perpendicular to it (assuming fiber alignment, if any, is in the forming direction)

Regression constants were determined as 0 for A and 73.1 for B with a coefficient of determination ( $r^2$ ) of 92%.



M151-297

Fig. 1. Compression stress-strain diagrams of various alignments and densities of flakeboard.

The regression equations used for Young's modulus and ultimate strength are:

$$x = e^{\mu}SG^{\alpha}SVR^{\beta} \tag{3}$$

in which  $x$  = property of interest (modulus of elasticity (MOE) or ultimate strength)  
 $\mu, \alpha, \beta$  = regression constants  
 SG = specific gravity

Table 1 lists the constants and the coefficients of determination for MOE and ultimate strength under tensile and compressive loading.

STRESS-STRAIN RESPONSE MODEL

Past attempts to characterize the nonlinear behavior of various materials have resulted in the presentation of numerous plausible equations having various levels

TABLE 1. Regression constants used in determining flakeboard strength and stiffness (Geimer 1980).

Regression constants	Ultimate strength		Modulus of elasticity	
	Tension	Compression	Tension	Compression
$\mu$	8.33	8.43	6.90	6.79
$\alpha$	1.59	2.06	1.59	1.39
$\beta$	1.14	0.75	1.31	1.27
$r^2$	96.2	92.7	94.8	95.3

of usefulness. A thorough summary of the more prominent curvilinear stress-strain formulations has been written by O'Halloran (1973) in his pursuit of an equation suitable to define the compression behavior of wood. Behavior of the flakeboard material can be described as being nearly asymptotic to failure (Fig. 1). O'Halloran asserts (1973) that the Ramberg-Osgood (R-O) equation is the most appropriate model to use when this asymptotic relationship is evident.

The R-O equation is a power relation of stress and modulus of elasticity to strain. A form of the equation is:

$$\epsilon = \frac{\sigma}{E} + K \left( \frac{\sigma}{E} \right)^n \quad (4)$$

in which  $\epsilon$  = strain (in./in.)  
 $E$  = modulus of elasticity (MOE) (psi)  
 $\sigma$  = stress (psi)  
 $K, n$  = derived constants

This expression has been widely used for characterizing the stress-strain behavior of nonlinear materials because of its versatility, ease of parameter definition, and its simple incorporation into computerized analyses. A shortcoming of this formulation is its inability to portray the perfectly plastic condition, but, unlike metals and plastics, wood-based materials seldom display this idealized behavior.

#### *Method of parameter definition*

Parameters for the R-O equation were determined for this preliminary assessment through use of a graphic technique. The MOE's of specimens tested under axial loading (i.e., tension or compression) were calculated by graphic slope construction techniques. Lines at slopes of  $m_1E$  and  $m_2E$  passing through the origin were then constructed on the stress-strain diagram (Fig. 2).

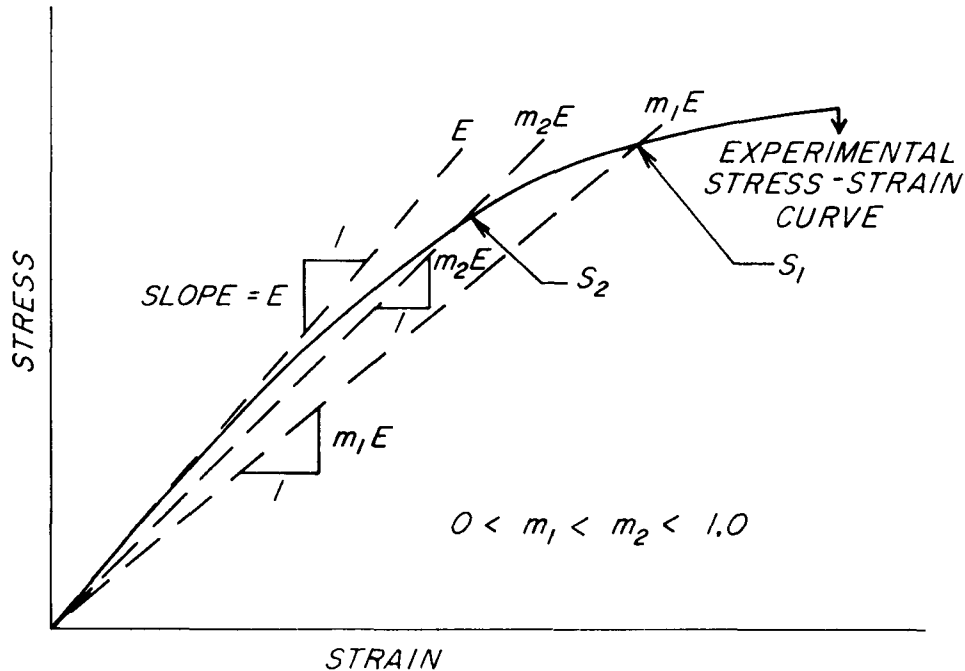
The constants  $m_1$  and  $m_2$  are chosen by three requirements. Both intersections of the line and the stress-strain plot must fall in the nonlinear portion of the plot (i.e.,  $m_1$  and  $m_2$  must be less than 1.0); these intersections should be separated by as large a strain as possible to obtain good definition of the R-O parameters while staying within that portion of the curve that is continuous; and, lastly,  $m_1$  must be less than  $m_2$ . The intersections of interest were labeled  $S_1$  and  $S_2$  corresponding to  $m_1$  and  $m_2$ , respectively.

The Ramberg-Osgood parameters can be defined as

$$n = 1 + \left\{ \frac{\log \left[ \frac{m_2 \left( \frac{1 - m_1}{1 - m_2} \right) \right]}{\log \frac{S_1}{S_2}} \right\} \quad (5)$$

and

$$K = \left( \frac{1}{m_1} - 1 \right) \left( \frac{S_1}{E} \right)^{1-n} \quad (6)$$



### M151-298

FIG. 2. Graphic construction for determination of Ramberg-Osgood parameters.

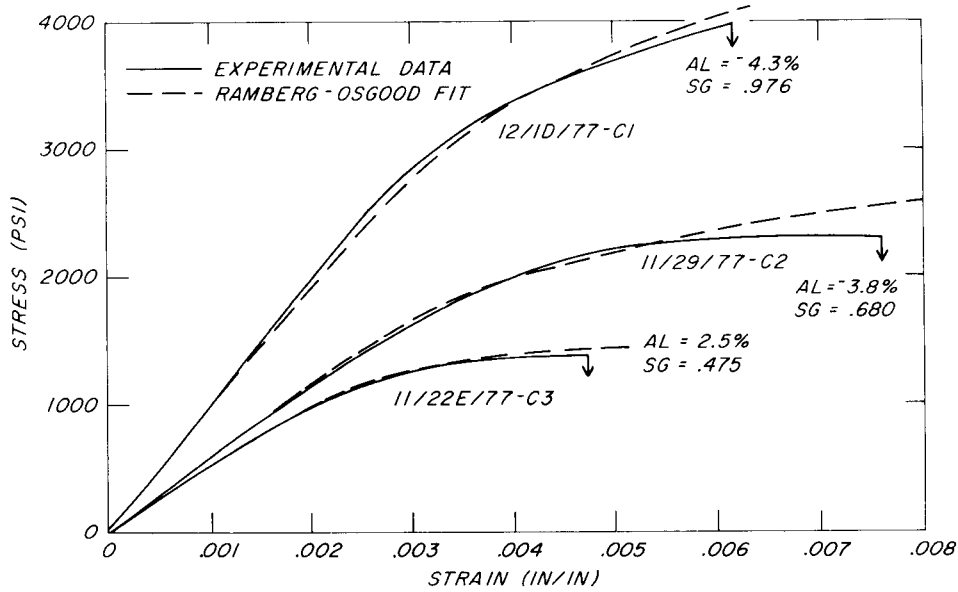
with the constraint assumed:  $0 < m_1 < m_2 < 1.0$   
 in which  $m_1$  and  $m_2$  = arbitrary constants

$S_1$  and  $S_2$  = stress values at intersections of the stress-strain plot and the lines at slopes of  $m_1E$  and  $m_2E$ , respectively.

Three examples of stress-strain curves were fitted by this method using  $m_1 = .70$  and  $m_2 = .85$  (Fig. 3). Theoretically, the linear-elastic portion of the test data should be exactly fitted by the R-O prediction. Errors in reading and plotting the initial slope cause cumulative errors evident in the example plots.

Values of the R-O constants  $K$  and  $n$  were sought that would provide an average representation of the stress-strain behavior to failure. Of primary importance in this study was the accuracy with which the failure strain is predicted. These constants were calculated for three levels of target fiber alignment ( $-80\%$ ,  $0\%$ ,  $+80\%$ ), four target density levels (30, 40, 50, 60 lb/ft<sup>3</sup>), and two stress states (uniaxial tension and compression). These average parameters (Table 2) were obtained by using Eqs. (5) and (6) with average values of  $S_1$ ,  $S_2$ , and  $E$ . Eight specimen stress-strain curves were examined to obtain each numerical average for the target random boards, and four specimens were available for defining the aligned parameters.

The parameters were, numerically, quite scattered due to their logarithmic-



M151-299

FIG. 3. Representative stress-strain diagrams and fitted Ramberg-Osgood functions.

based derivation (Table 2). The sensitivity of the equation parameters was further reduced by averaging the  $S_1$  and  $S_2$  and  $E$  values over all density classes.

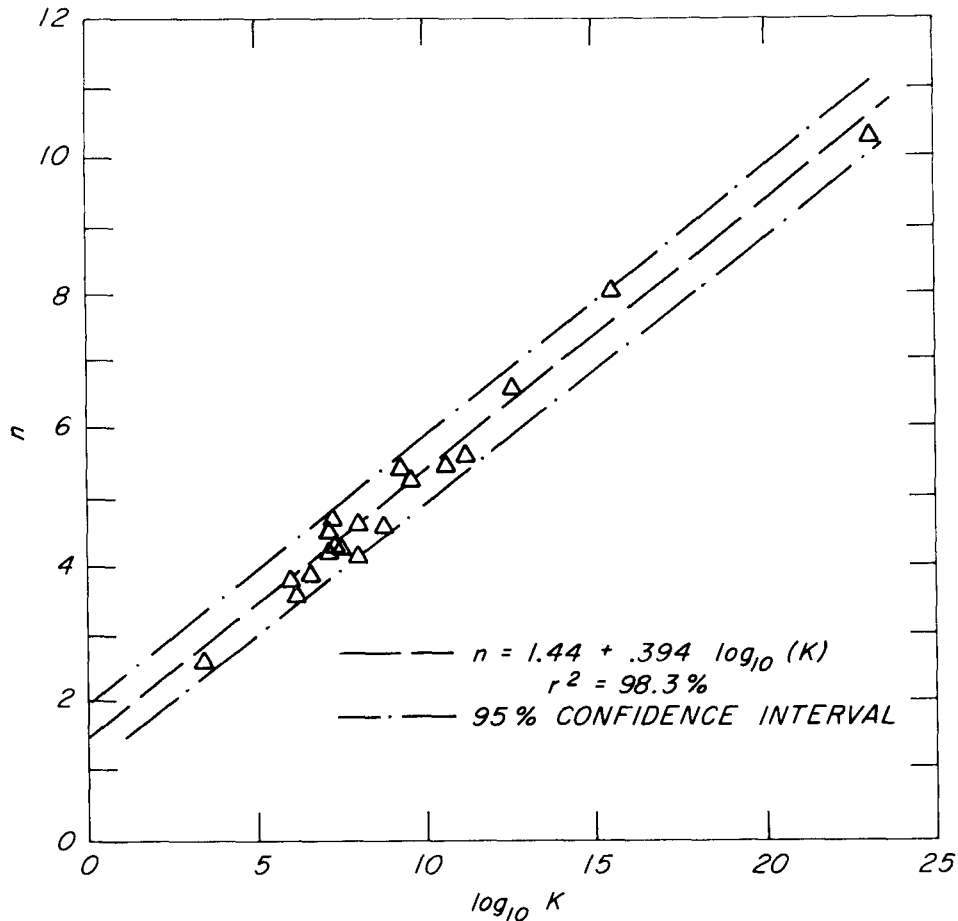
*Variability analysis*

Accurate prediction of flakeboard stress-strain behavior to failure requires not only forecasting strain levels for intermediate load levels but also failure strain at the ultimate stress condition. As this study was intended only as an assessment of a modeling technique, and not as the basis for design requirements, estimates of variability were generated only to illustrate the quality of fit expected for this family of materials.

TABLE 2. Average Ramberg-Osgood parameters  $n$  and  $K$  for various classes of flakeboard of 0.020- x 3.0-inch Douglas-fir disk flakes.

Target alignment (%)	Parameters at target densities of								Parameters at all densities	
	30 lb/ft <sup>3</sup>		40 lb/ft <sup>3</sup>		50 lb/ft <sup>3</sup>		60 lb/ft <sup>3</sup>			
	$n$	$K$	$n$	$K$	$n$	$K$	$n$	$K$	$n$	$K$
TENSION										
-80	— <sup>1</sup>	—	6.52	$4.23 \times 10^{12}$	4.26	$1.64 \times 10^7$	3.55	$1.02 \times 10^8$	4.37	$4.79 \times 10^7$
0 (random)	8.02	$3.09 \times 10^{15}$	4.23	$1.95 \times 10^7$	2.57	2,970	4.31	$2.18 \times 10^7$	6.11	$2.14 \times 10^{11}$
+80	—	—	10.52	$1.17 \times 10^{23}$	—	—	4.15	$1.00 \times 10^8$	5.93	$4.58 \times 10^{11}$
COMPRESSION										
-80	4.23	$1.31 \times 10^7$	5.38	$1.46 \times 10^9$	4.69	$1.83 \times 10^7$	4.54	$1.10 \times 10^7$	4.71	$4.43 \times 10^7$
0 (random)	4.28	$1.61 \times 10^7$	4.07	$9.58 \times 10^6$	3.82	$8.69 \times 10^5$	5.20	$3.49 \times 10^9$	4.60	$1.10 \times 10^8$
+80	4.57	$5.98 \times 10^6$	3.88	$3.40 \times 10^6$	5.48	$3.56 \times 10^{10}$	5.65	$1.34 \times 10^{11}$	5.46	$1.76 \times 10^9$

<sup>1</sup> Stress-strain curves unavailable.



M151-300

FIG. 4. Correlation between Ramberg-Osgood parameters.

The individual stress-strain plots of Fig. 3 provide visual evidence of the R-O technique's versatility in characterizing an asymptotic set of data points. By digitizing the data, errors in measuring the initial slope become nonexistent with subsequent improvements in fitting of the nonlinear data. The ability to provide a low-error fit for one stress-strain curve is nearly meaningless for a material with as many processing variables as a structural flakeboard. For this reason, variability in fitting a number of curves simultaneously was of consideration.

Calculation of the R-O parameters  $K$  and  $n$  for a number of stress-strain curves has shown these parameters to be extremely variable. This variability is such that two essentially identical curves will have parameters whose values differ widely, yet each set of parameters could be interchanged without having any significant effect upon the predictive capability of each individual curve. In short, a study of the variability of the R-O parameters would not yield any information as to the suitability of the R-O function as a prediction equation.

TABLE 3. Modified coefficients of determination using Ramberg-Osgood (R-O) and linear-elastic (L-E) ultimate strain predictions.

Prediction equation for target alignments from Table 2 over all densities		$\bar{r}^2$ for target alignment <sup>1</sup> of				All alignments
		0%	$\pm 40\%$	$\pm 60\%$	$\pm 80\%$	
TENSION						
-80%	R-O	0.9638	0.9720	0.9618	0.8957	0.9507
	L-E	0.8818	0.8189	0.8023	0.8516	0.8380
0 (random)	R-O	0.9307	—	—	—	—
	L-E	0.8818	—	—	—	—
+80%	R-O	0.8706	0.8857	0.9689	0.8594	0.8876
	L-E	0.8818	0.8984	0.9437	0.9792	0.9048
COMPRESSION						
-80%	R-O	0.9128	0.8407	0.9256	0.8860	0.8881
	L-E	0.8864	0.7159	0.7860	0.7593	0.7705
0 (random)	R-O	0.9386	—	—	—	—
	L-E	0.8864	—	—	—	—
+80%	R-O	0.9268	0.8433	0.9418	0.8336	0.8871
	L-E	0.8864	0.8390	0.9387	0.8316	0.8774

<sup>1</sup> Values were obtained using negative target alignment test data with -80% parameters and positive target alignment test data with +80% parameters.

An attempt was made to compute the R-O parameters by using an iterative least-squares procedure (Dixon and Brown 1977) on pooled stress-strain data from a family of specimens (i.e., equal target alignment and density). As the form of the desired nonlinear regression was known, the sum of the squares of the residuals was the quantity to be minimized by selection of appropriate parameters. This effort was unsuccessful in achieving convergence on a set of parameters for a given data set. The one reason suggested for this behavior was a high degree of correlation between the equation parameters  $K$  and  $n$ .

To assess the relationship between the equation parameters, the parameter values obtained by graphical techniques were plotted (Fig. 4). A linear correlation between  $n$  and the base-10 logarithm of  $K$  would be appropriate if the values of  $S_1/E$  and  $S_1/S_2$  were linearly correlated (Eqs. 5 and 6).

Regression of the graphically obtained data pairs yielded this equation:

$$N = 1.44 + 3.94 \log_{10}(K) \quad (7)$$

$$(r^2 = 0.982)$$

The coefficient of determination and the 95% confidence interval (Fig. 4) indicate the quality of the relationship. Correlation between these parameters indicates that any subsequent nonlinear regression attempts based on iterative techniques would be fruitless.

An evaluation was made of the accuracy that could be expected in predicting ultimate strain when using the graphically determined parameters in Table 2. A simple substitution of Eqs. (2) and (3) into Eq. (4) with the appropriate regression



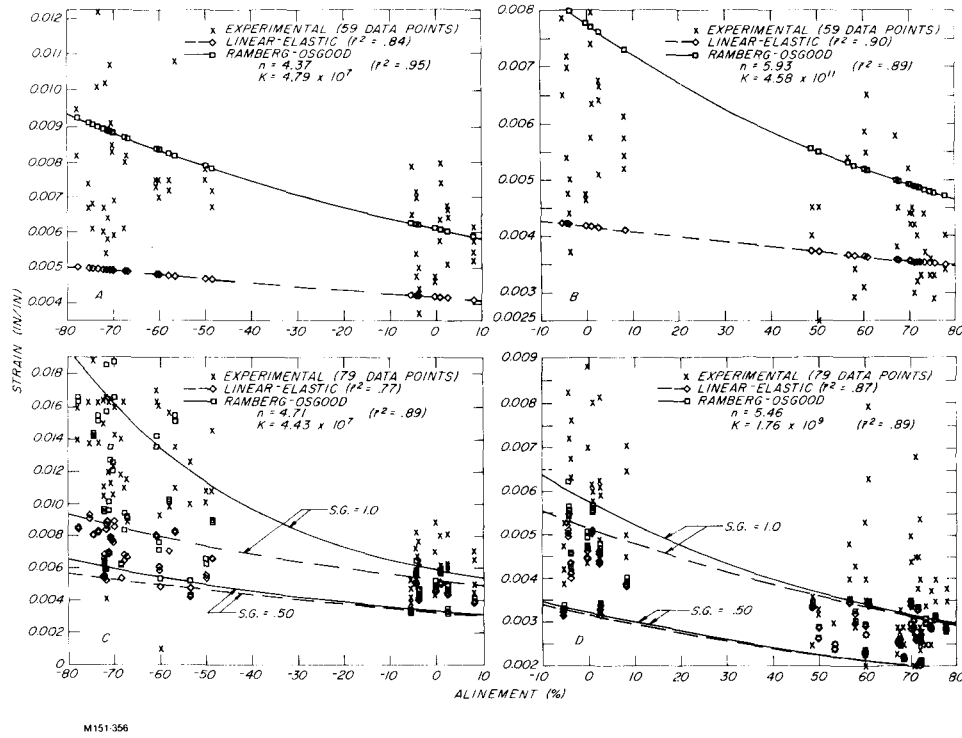


FIG. 5. Predicted and observed ultimate strains. a) Tensile loading with alignment  $\leq 0$ . b) Tensile loading with alignment  $\geq 0$ . c) Compressive loading with alignment  $\leq 0$ . d) Compressive loading with alignment  $\geq 0$ .

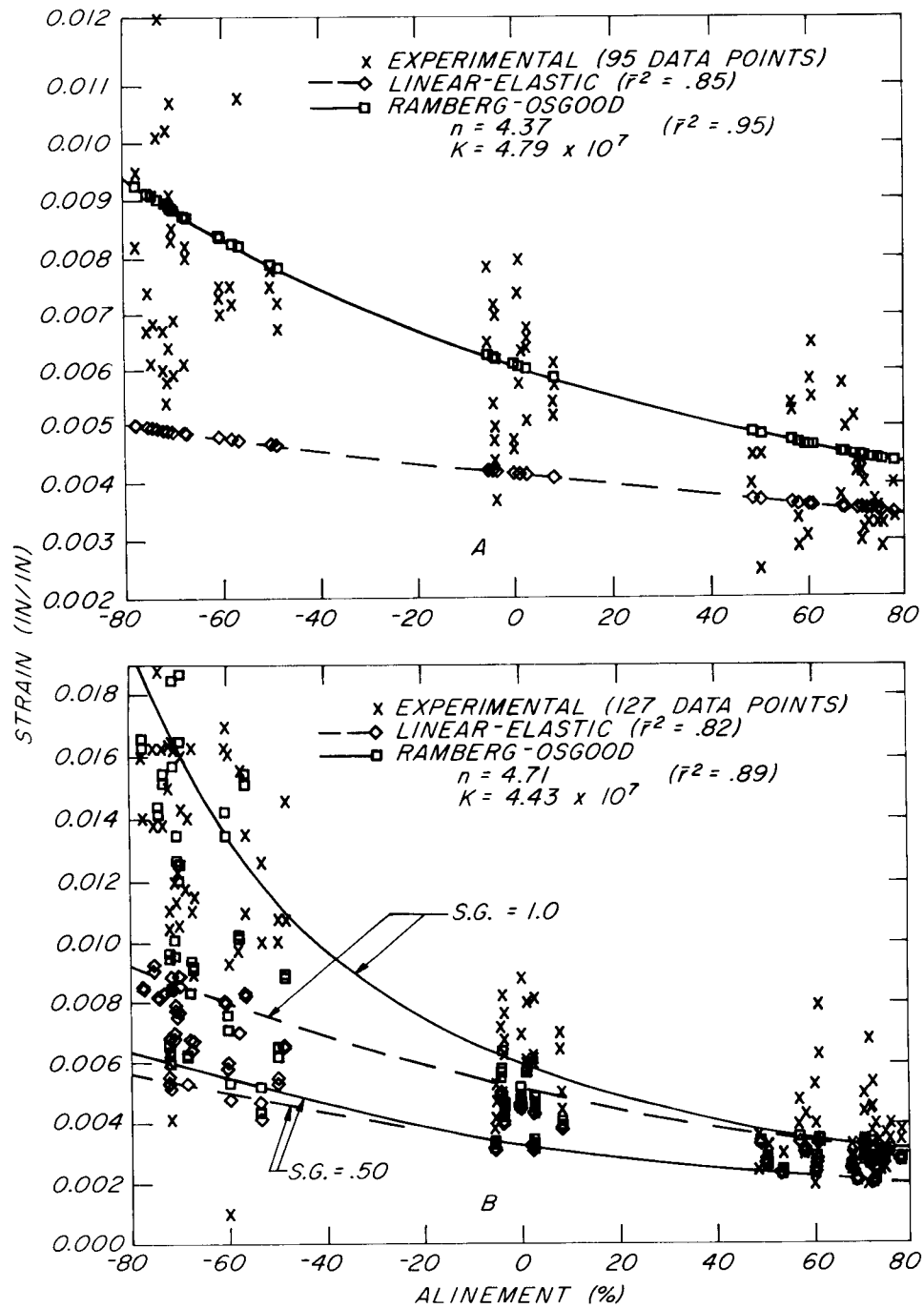
constants and R-O parameters yields predictions of linear-elastic (L-E) and R-O predicted ultimate strains (Table 3). The L-E ultimate strain is simply the ultimate stress divided by MOE, both quantities determined through use of the regression constants of Table 1. To measure the quality of fit, a modified coefficient of determination ( $\bar{r}^2$ ) was calculated. This modification was necessary because the function is forced through the origin, thus

$$\bar{r}^2 = \frac{\sum y^2 - \sum e^2}{\sum y^2}$$

in which  $\sum e^2$  = the sum of the residual squared,  $\sum(Y_{\text{experimental}} - Y_{\text{predicted}})^2$ , and  $\sum y^2$  = the sum of the experimental values squared

Each of the R-O parameter pairs derived for all densities in Table 2 was used to calculate coefficients of determination (Table 3) for each class of materials used to derive the prediction parameters. Each parameter pair was checked for accuracy with other classes of alignment data.

The coefficients indicate that all of the R-O equations (except the +80% alignment, tension-state prediction) provided more accurate results than did the L-E



M151-357

FIG. 6. Predicted and observed ultimate strain over entire alignment range. a) Tensile loading. b) Compressive loading.

analyses (Table 3). The accuracy was significantly better for data from specimens with negative alignment using the  $-80\%$  parameters, moderately improved using the random parameters, and only slightly, if at all, improved for positive-alignment data using the  $+80\%$  prediction parameters. The coefficient of determination for pooled data from the random tests through the  $\pm 80\%$  alignment indicates the overall ability of each equation to predict ultimate strains over the broad range of alignments (Table 3). Observations and predictions for two ranges of target alignment (0 to  $+80\%$  and 0 to  $-80\%$ ) and two stress states are plotted in Fig. 5. The ultimate strain for tension-testing predictions (Fig. 5a, b) falls on a single line. This is caused by equal regression coefficients,  $\alpha$  (Table 1). The compression strains (Fig. 5c, d) demonstrate the effect of the specific gravity parameter on the predicted behavior.

Of special note are the R-O predictions in Fig. 5b. The parameters depicted were calculated from only eight specimens in the  $+80\%$  alignment class and, subsequently, do not fit any of these data well. Additionally, the L-E predictions are slightly better than the R-O. This indicates that reduction of the parameters would definitely improve the fit, considering that the degenerate case (with  $n = 0$ ) is the L-E solution. Using this rationale, the R-O parameters calculated for the  $-80\%$  alignment class were evaluated using the observations ranging from  $-80\%$  to  $+80\%$  alignment (Fig. 6a (tension) and 6b (compression)). Coefficients of determination,  $\bar{r}^2$  (Fig. 6), allow direct comparison of the R-O and L-E predictions. An improved fit is obtained for the tension data using just one set of parameters and the quality of fit of the compression data is not degraded.

#### CONCLUSIONS

A reduction in the number of parameters necessary to characterize the nonlinear behavior of flakeboard was required to provide a usable relationship.

Though the small amount of data used to define the R-O parameters in this study precludes any further generalizations about the parameter quantities, this work identifies the improvements possible in defining material failure strains using a nonlinear relationship. Definition of the ultimate strain for flakeboards will provide a means of evaluating failures in plate structures in terms of curvatures, not stresses. Design of multilayer structural flakeboards to meet minimum strength requirements will require designers to recognize the nonlinear stress-strain properties of this material in their analyses and to generate a failure criterion that is usable in light of this nonlinearity.

The ultimate strain predictions made in this study with a nonlinear characterization proved to be accurate over all ranges of alignment and density with a minimum number of parameters required in the analyses. Poor resolution of ultimate strain by linear-elastic analyses was especially apparent for flakeboard materials in compression with randomized flakes or flakes aligned perpendicular to the stress direction.

#### REFERENCES

- BRUMBAUGH, J. 1960. Effect of flake dimensions on properties of particleboards. *For. Prod. J.* 10(5):243-246.
- DICKERHOOF, H. E., AND D. B. MCKEEVER. 1980. Resource potential for waferboard production in

